HOKKAIDO UNIVERSITY

Title	Direct renin inhibitor ameliorates insulin resistance by improving insulin signaling and oxidative stress in the skeletal muscle from post-infarct heart failure in mice
Author(s)	Fukushima, Arata; Kinugawa, Shintaro; Takada, Shingo; Matsumoto, Junichi; Furihata, Takaaki; Mizushima, Wataru; Tsuda, Masaya; Yokota, Takashi; Matsushima, Shouji; Okita, Koichi; Tsutsui, Hiroyuki
Citation	European journal of pharmacology, 779, 147-156 https://doi.org/10.1016/j.ejphar.2016.03.022
Issue Date	2016-05-15
Doc URL	http://hdl.handle.net/2115/65354
Rights	© 2016. This manuscript version is made available under the CC-BY-NC-ND 4.0 license http://creativecommons.org/licenses/by-nc-nd/4.0/
Rights(URL)	http://creativecommons.org/licenses/by-nc-nd/4.0/
Type	article (author version)
File Information	EurJPharmacol779_147.pdf

Direct renin inhibitor ameliorates insulin resistance by improving insulin signaling and oxidative stress in the skeletal muscle from post-infarct heart failure in mice

Arata Fukushima [a], Shintaro Kinugawa [a], Shingo Takada [a], Junichi Matsumoto [a], Takaaki Furihata [a], Wataru Mizushima [a], Masaya Tsuda [a], Takashi Yokota [a], Shouji Matsushima [a], Koichi Okita [b], and Hiroyuki Tsutsui [a]

[a] Department of Cardiovascular Medicine, Hokkaido University Graduate School of Medicine, Sapporo, Japan

[b] Graduate School of Lifelong Sport, Hokusho University, Ebetsu, Japan

Address for Correspondence:

Shintaro Kinugawa, MD, PhD.

Department of Cardiovascular Medicine

Hokkaido University Graduate School of Medicine

Kita-15, Nishi-7, Kita-ku, Sapporo 060-8638, Japan

Phone: +81-011-706-6973   Fax: +81-011-706-7874

E-mail:tuckahoe@med.hokudai.ac.jp

Abstract

Insulin resistance can occur as a consequence of heart failure (HF). Activation of the renin-angiotensin system (RAS) may play a crucial role in this phenomenon. We thus investigated the effect of a direct renin inhibitor, aliskiren, on insulin resistance in HF after myocardial infarction (MI). MI and sham operation were performed in male C57BL/6J mice. The mice were divided into 4 groups and treated with sham-operation (Sham, n=10), sham-operation and aliskiren (Sham+Aliskiren; 10 mg/kg/day, n=10), MI (n=11), or MI and aliskiren (MI+Aliskiren, n=11). After 4 weeks, MI mice showed left ventricular dilation and dysfunction, which were not affected by aliskiren. The percent decrease of blood glucose after insulin load was significantly smaller in MI than in Sham ($14\pm5\%$ vs. $36\pm2\%$), and was ameliorated in MI+Aliskiren ($34\pm5\%$) mice. Insulin-stimulated serine-phosphorylation of Akt and glucose transporter 4 translocation were decreased in the skeletal muscle of MI compared to Sham by 57% and 69%, and both changes were ameliorated in the MI+Aliskiren group (91% and 94%). Aliskiren administration in MI mice significantly inhibited plasma renin activity and angiotensin II (Ang II) levels. Moreover, (pro)renin receptor expression and local Ang II production were upregulated in skeletal muscle from MI and were attenuated in MI+Aliskiren mice, in tandem with a decrease in superoxide production and NAD(P)H oxidase activities. In conclusion, aliskiren ameliorated insulin resistance in HF by improving insulin signaling in the skeletal muscle, at least partly by inhibiting systemic and (pro)renin receptor-mediated local RAS activation, and subsequent NAD(P)H oxidase-induced oxidative stress.

Keywords: Direct renin inhibitor, insulin resistance, heart failure, skeletal muscle, oxidative stress, (pro)renin receptor

1. Introduction

Insulin resistance is highly prevalent and an established risk factor for heart failure (HF), and it has been associated with reduced functional capacity and poor prognosis (Doehner et al., 2005; Ingelsson et al., 2005; Lopaschuk et al., 2010). Conversely, HF itself is known to trigger the occurrence of insulin resistance, accounting for a vicious cycle of functional exacerbation of these two conditions (AlZadjali et al., 2009; Witteles et al., 2004). Indeed, the peripheral effects of insulin resistance are likely to represent a major metabolic feature of the pathophysiology of HF, contributing to key clinical symptoms such as breathlessness and early muscle fatigue (Kinugawa et al., 2015; Okita et al., 2013; Wilson et al., 1993). Multiple mechanisms of insulin resistance have already been identified, including increased oxidative stress and hyperactivation of the renin-angiotensin system (RAS) (Officers et al., 2002; Wei et al., 2006). We previously reported that insulin resistance was induced in experimental HF in mice (Ohta et al., 2011), and a later study showed that this induction was accompanied by increased local angiotensin II (Ang II) in the skeletal muscle and subsequent NAD(P)H oxidase-derived oxidative stress (Fukushima et al., 2014). In addition, the recent discovery of a (pro)renin receptor for renin and its precursor, prorenin, raises the possibility that these components of RAS may play significant pathophysiological roles in the insulin resistance of rats with high fructose diet-induced diabetes or in post-infarct HF mice (Fukushima et al., 2014; Nagai et al., 2009).

Aliskiren is a potent direct renin inhibitor that blocks the first rate-limiting step in RAS, preventing the compensatory rise in plasma renin activity and other

downstream components of this system from occurring during angiotensin converting enzyme (ACE) inhibitor or Ang II receptor blocker treatment (Gradman and Traub, 2007). Aliskiren has been shown to protect against the development of insulin resistance in an animal model of diabetes by improving skeletal muscle glucose transport as well as to improve insulin sensitivity in hypertensive patients with metabolic syndrome (Fogari et al., 2010; Iwai et al., 2010; Marchionne et al., 2012). In addition, it has been reported that aliskiren can inhibit the free form of mature renin and the (pro)renin receptor-bound forms of renin and prorenin, suggesting that these dual inhibitory effects play roles in both systemic RAS and (pro)renin receptor-mediated tissue RAS (Biswas et al., 2010). To date, clinical trials to investigate the effect of aliskiren on myocardial infarction (MI) and HF have failed to improve outcomes by administration of aliskiren in combination with an ACE inhibitor or Ang II receptor blocker (Gheorghiade et al., 2013; Solomon et al., 2011). However, it remains to be determined whether low-dose single treatment with aliskiren could ameliorate the insulin resistance associated with MI and HF.

In the present study, we examined the effects of aliskiren on the insulin resistance and the insulin signaling in the skeletal muscle from post-infarct HF mice, mainly focusing on its effects on the (pro)renin receptor-mediated tissue RAS and oxidative stress in the skeletal muscle.

2. Materials and methods

All procedures and animal care were approved by our institutional animal research committee and conformed to the Guidelines for the Care and Use of Laboratory Animals of the Hokkaido University Graduate School of Medicine.

2.1. Experimental animals

Male C57BL/6J mice, 8 to 10 weeks old and 20 to 21 g body weight (BW), were maintained on a normal diet (CE-2; CLEA Japan, Tokyo) containing 4.2% fat and 54.6% carbohydrate. MI was established by ligating the left coronary artery as described previously (Fukushima et al., 2014; Kinugawa et al., 2000). Sham operation without ligation of the coronary artery was also performed. Each group of mice was then randomly divided into 2 groups, a group with and a group without aliskiren (10 mg/kg BW/day; Novartis Pharmaceuticals, Basel, Switzerland) administered subcutaneously for 4 weeks using an osmotic minipump (model 2004; Alzet, Palo Alto, CA). The non-depressor concentration of aliskiren was chosen on the basis of our preliminary data of blood pressure measurement by using the indirect tail-cuff method (MK-1030; Muromachi Kikai Co., Ltd., Tokyo, Japan) (**Supplementary material**). Experiments were performed at 4 weeks after operation in the following 4 groups: Sham (n=10), Sham+Aliskiren (n=10), MI (n=11), and MI+Aliskiren (n=11).

2.2. Echocardiographic and hemodynamic measurements

Echocardiographic and hemodynamic measurements were performed under light anesthesia with tribromoethanol/amylene hydrate (avertin; 2.5% wt/vol, 8 μl/g BW

ip), which has short duration of action and modest cardiodepressive effects and spontaneous respiration, as described previously (Fukushima et al., 2014; Ohta et al., 2011). Standard echocardiographic short- and long-axis views were obtained at the levels of the papillary muscles. Left ventricular function, ventricular size and wall thickness were measured from M-mode frames at a paper speed of 50 mm/s. To perform hemodynamic measurements, a 1.4 Fr micromanometer-tipped catheter (Millar Instruments, Houston, TX) was inserted into the right carotid artery and then advanced into the left ventricle (LV) to measure LV pressures.

2.3. Tissue preparation and organ histology

Heart, lung, and hindlimb skeletal muscle including the quadriceps, gastrocnemius, and soleus were excised 3 min after intraperitoneal injection of saline, with or without human regular insulin (1.0 U/kg BW) and weighed under deep anesthesia with avertin (2.5% wt/vol, 10 μl/g BW, ip). To determine the infarct size, myocyte cross-sectional area, and total collagen volume in cardiac tissue, ventricular tissue was fixed in 6% formaldehyde, cut into three transverse sections—the apex, middle ring, and base—and stained with hematoxylin-eosin or Masson's trichrome as described previously (Matsushima et al., 2009; Sobirin et al., 2012).

2.4. Plasma biochemical measurement

After the animals were fasted for 8 h, blood samples were collected from the inferior vena cava, the blood glucose level was determined using a glucometer (Glutest Ace R; Sanwa Kagaku Kenkyusho, Nagoya, Japan) and the plasma insulin was measured by an ELISA kit (Morinaga Institute, Kanagawa, Japan). The homeostasis

model assessment index (HOMA-IR) was calculated using the formula of fasting glucose (mmol/l) × fasting insulin (mU/l)/22.5. Total cholesterol, triglyceride, and nonesterified fatty acid (NEFA) were measured by a commercial ELISA kit (Wako Pure Chemical Industries, Osaka, Japan). The plasma renin activity level was determined using a SensoLyte 520 Renin Assay Kit (AnaSpec Inc., San Jose, CA). The plasma angiotensin (Ang) II level was measured by using an enzyme immunoassay (EIA) kit (Phoenix Pharmaceuticals Inc., Burlingame, CA) as previously described (Fukushima et al., 2014).

2.5. *Intraperitoneal insulin tolerance test*

For the insulin tolerance test, mice were injected intraperitoneally with human regular insulin (0.5 U/kg BW) and blood samples were collected before and 15, 30, 45, 60, 90, and 120 min after the injection. Blood glucose levels were determined using a glucometer (Glutest Ace R; Sanwa Kagaku Kenkyusho, Nagoya, Japan) (Takada et al., 2014). Data are shown as a percent change in blood glucose levels after insulin load.

2.6. *Western blot analysis*

Forty milligrams of frozen quadriceps skeletal muscle tissue was homogenized for 30 s with a Polytron homogenizer in a homogenization buffer containing 20 mM $NaHCO_3$, pH 7.0, 0.25 M sucrose, 5 mM NaN_3, 1 mM leupeptin, 1 mM aprotinin, and 1 mM pepstatin) at 4°C. Twenty μg of denatured proteins was subjected to 8-12% SDS-PAGE on a polyvinylidene difluoride (PVDF) membrane as previously described (Takada et al., 2013). After blocking in 5% fat-free milk for 1 h, the membranes were probed with the following antibodies: ATP6P2/(pro)renin receptor (Abcam Inc.,

Cambridge, MA), Akt, phosphoserine Akt (Ser473), and glucose transporter 4 (GLUT4)

(Cell Signaling Technology, Beverly, MA). The membranes were then incubated with

the appropriate secondary antibodies (Santa Cruz Biotechnology, Santa Cruz, CA) for 1

h. These bands were visualized by enhanced chemiluminescence and quantified with

Image J software (NIH, Bethesda, MD). The resulting values were expressed as the ratio

of target band intensity to total protein or internal control intensity. GAPDH (Cell

Signaling Technology) was used as an internal control to normalize the results and to

control for blot-to-blot variation. Translocation of GLUT4 was also measured by the

methods described previously (Fukushima et al., 2014; Mohammad et al., 2006). In

short, subcellular membrane fractions were prepared by sequential differential

centrifugation. The homogenate of quadriceps skeletal muscle was centrifuged at $1,200g$

for 10 min to remove debris. The supernatant was then centrifuged at $9,000g$ for 10 min

to allow mitochondria and nuclei to sediment. The resultant supernatant was centrifuged

at $190,000g$ for 2 h at 4°C, yielding a pellet of total membrane fraction and the

remaining supernatant, which was designated the cytosol fraction. The membrane and

the cytosol fractions (20 µg each lane) were subjected to immunoblot analysis as

described above. GLUT4 translocation was assessed by the ratio of the membrane

fraction to the cytosol fraction of total GLUT4 protein.

2.7.   Quantitative reverse transcriptase PCR

Total RNA was extracted from hindlimb skeletal muscle tissues including the

quadriceps and soleus in the 4 groups of mice with QuickGene-810 (FujiFilm, Tokyo,

Japan) according to the manufacturer's instructions. The extracted total RNA (2 µg) was

reverse-transcribed with a high capacity cDNA reverse transcription kit (Applied

Biosystems, Foster City, CA). Real-time quantitative RT-PCR was performed by using

a 7300 real-time PCR system (Applied Biosystems) to amplify samples for

angiotensinogen (Mm00599662_m1), ACE (Mm00802048_m1), Ang II type1 receptor

(Mm00507771_m1), cathepsin D (Mm00515586_m1), ATP6AP2/(pro)renin receptor

(Mm00510396_m1), p47^{phox} (Mm00447921_m1), p22^{phox} (Mm00514478_m1), and

Nox2 (Mm01287743_m1) cDNA in the skeletal muscle. Relative mRNA was analyzed

using a comparative $2^{-\Delta\Delta CT}$ method, and normalized to GAPDH as the internal control.

2.8.   *Immunohistochemistry for (P)RR*

      Quadriceps skeletal muscle tissues were fixed with 4% paraformaldehyde at 4°C,

and were immersed in 1% H_2O_2 in methanol to inhibit endogenous peroxidase. The

sections were incubated with anti-ATP6P2/(pro)renin receptor antibody (Abcam Inc.) as

a primary antibody, and then reacted with biotin-conjugated anti-rabbit IgG as the

secondary antibody (DAKO, Carpinteria, CA). Immunohistochemical reactions were

visualized by using a standard kit [3,3'-diaminobenzidine tetrahydrochloride (DAB);

DAKO, CA, USA] as previously described (Fukushima et al., 2014; Satofuka et al.,

2007).

2.9.   *Measurement of Ang II content in the skeletal muscle*

      Ang II content in the skeletal muscle tissues was measured as previously

described (Fukushima et al., 2014). Briefly, homogenates of quadriceps skeletal muscle

tissues were centrifuged at 15,000*g* for 20 min, and the supernatant was loaded on an

equilibrated Sep-Pak C18 cartridge (Millipore, New York, NY), eluted with buffer

(60% acetonitrile in 1% trifluoroacetic acid), and collected in a centrifuge tube. The

eluant was then evaporated by using a centrifugal concentrator (Savant Speedvac, Thermo Scientific, Japan). Ang II content was determined using an EIA kit (Phoenix Pharmaceuticals Inc.) (de Resende et al., 2006).

2.10. Superoxide (O_2^-) production and NAD(P)H oxidase activity

The chemiluminescence elicited by O_2^- in the presence of lucigenin (5 µmol/l) was determined in quadriceps skeletal muscle tissues using a luminometer (AccuFLEX Lumi 400; ALOKA, Tokyo, Japan), as previously described (Takada et al., 2013; Yokota et al., 2009). The measurements were also performed in the presence of tiron (20 mmol/l), a cell-permeant, nonenzymatic scavenger of O_2^- to validate the chemiluminescence signals. NAD(P)H oxidase activity was examined in the homogenates from quadriceps skeletal muscle by the lucigenin assay after the addition of NAD(P)H (300 µmol/l).

2.11. Statistical analysis

Data are represented as the means±S.E.M. Comparisons were performed using a one-way ANOVA followed by the Tukey's multiple-comparison test whenever differences were detected. Survival analysis was performed by the Kaplan-Meier method, and between-group differences in survival were tested using the log-rank test. In the intraperitoneal insulin tolerance test, differences between groups were determined with repeated-measures ANOVA. A value of $P < 0.05$ was considered statistically significant.

3. Results

3.1.   Effect of aliskiren on mortality rates and cardiac dysfunction after MI

The mortality rate up to 4 weeks after operation was significantly lower in the

MI+Aliskiren group compared to the MI group (16.8% vs. 46.2%, P < 0.01). No mice

died after sham operation. **Table 1** shows animal characteristics in the 4 groups of mice.

The heart weight and lung weight/BW were significantly higher in MI compared to

Sham mice. There was no difference in the weights of skeletal muscle, including the

quadriceps, gastrocnemius, and soleus, among the 4 groups. The echocardiographic and

hemodynamic data are also shown in **Table 1**. There were no significant differences in

heart rate and mean aortic pressure among the 4 groups. MI mice exhibited greater LV

diameters and lower LV fractional shortening than Sham mice. LV end-diastolic

pressure (LVEDP) was significantly elevated, and both LV + and – dP/dt were

decreased in MI mice compared to Sham mice. Consistent with the hemodynamic data,

histopathological analysis revealed that the infarct size, myocyte cross-sectional area,

and collagen volume fraction were all higher in MI compared to Sham mice (**Table 1**

and Fig. 1A, B). Treatment with aliskiren tended to attenuate LV dilatation and infarct

size, to elevate end-diastolic pressure, and to improve systolic function in MI mice.

However, there were no statistically significant differences in these parameters between

the MI and MI+Aliskiren groups. In addition, aliskiren treatment did not affect these

parameters in Sham mice (**Table 1**)

3.2.   Effect of aliskiren on insulin resistance in post-infarct HF mice

Fasting blood glucose levels were not different among the 4 groups, but the

fasting plasma insulin levels were higher in MI mice than Sham mice and were

normalized in the MI+Aliskiren group (**Table 2**). The HOMA index, an index of insulin

resistance, was therefore greater in the MI than the Sham group and was also

normalized in the MI+Aliskiren group (**Table 2**). Consistent with our previous study

(Fukushima et al., 2014), the percent decrease of blood glucose 30 and 45 min after

insulin load, as well as the area under the curve (AUC) of glucose response after insulin

load, was significantly smaller in MI mice than Sham mice (**Fig. 2A, B**). Importantly,

aliskiren administration significantly enhanced the decrease in blood glucose after

insulin load in MI. Collectively, these results suggest that insulin resistance occurs in

MI mice and can be ameliorated by aliskiren treatment. There were no significant

differences in the percent change of blood glucose after glucose load and the AUC

among the 4 groups (**Supplementary material**). In addition, aliskiren did not affect

these parameters in Sham mice (**Fig. 2A, B**). The other biochemical measurements are

shown in **Table 2**. There were no differences in total cholesterol or triglyceride among

the 4 groups. NEFA was higher in the MI than the Sham animals, and this difference

was normalized by aliskiren treatment. Furthermore, the mean adipocyte area in

epididymal adipose tissue was not significantly changed among the 4 groups

(**Supplementary material**).

3.3.   Effect of aliskiren on insulin signaling in the skeletal muscle

There were no significant differences in the total or tyrosine phosphorylated

protein levels of IR-β, IRS-1, and PI3-kinase in insulin-stimulated skeletal muscle

among the 4 groups (**Supplementary material**). In contrast, serine-phosphorylation of

Akt in insulin-stimulated skeletal muscle was lower in the MI than the Sham mice, and

was improved in the MI+Aliskiren group (**Fig. 3A**). Consistently, GLUT4 translocation

from the cytosol to plasma membrane was significantly lower in MI mice compared to their Sham counterparts, and was normalized in the MI+Aliskiren mice (**Fig. 3B**). No significant differences in the total or phosphorylated protein levels of insulin signaling were observed in insulin-unstimulated skeletal muscle among the 4 groups (data not shown).

3.4.   Effect of aliskiren on circulating RAS

Both plasma renin activity and Ang II levels were significantly higher in MI mice than Sham mice and were inhibited in MI+Aliskiren mice (**Fig. 4A, B**).

3.5.   Effect of aliskiren on (pro)renin receptor in the skeletal muscle

Cathepsin D (a surrogate marker for renin), angiotensinogen, ACE, and Ang II type1 receptor mRNA levels in the skeletal muscle were all comparable among the 4 groups (**Fig. 5**). In contrast, the gene expression and protein levels of (pro)renin receptor were both higher in the skeletal muscle of MI compared to Sham mice, and these increases were inhibited in the MI+Aliskiren group (**Fig. 5 and Fig. 6A**). Similarly, positive immunohistochemical staining for (pro)renin receptor was higher in skeletal muscle cells from MI than Sham mice, and was attenuated in the MI+Aliskiren group (**Fig. 6A**). Since upregulated (pro)renin receptor expression has been shown to potentiate local RAS activation, we next examined Ang II content in the skeletal muscle. As we expected, Ang II content was also higher in the skeletal muscle from MI mice compared to Sham mice, and the increment was significantly suppressed by aliskiren treatment (**Fig. 6B**).

3.6.   Effect of aliskiren on oxidative stress in the skeletal muscle

Both O_2^- production and NAD(P)H oxidase activities were significantly higher in the skeletal muscle of MI than Sham mice, and these increases were inhibited in MI+Aliskiren mice (**Fig. 7A**). Consistent with these activities, the NAD(P)H oxidase subunits, NOX2, p22^{phox}, and p47^{phox} mRNA levels were all higher in the MI than the Sham group, and these increases were significantly inhibited by aliskiren (**Fig. 7B**).

4. Discussion

The major findings of present study are that the administration of aliskiren into post-infarct HF mice ameliorates both systemic insulin resistance and impaired insulin signaling in the skeletal muscle, concomitant with an inhibition of NAD(P)H oxidase – induced O_2^- production. Moreover, aliskiren treatment attenuates an increase in (pro)renin receptor expression and subsequent Ang II production in the skeletal muscle, in addition to attenuating the increases in circulating renin activity and Ang II levels. Therefore, the salutary effect of aliskiren treatment on the insulin resistance in HF mice is likely due to the inhibition of both systemic RAS and (pro)renin receptor-mediated local RAS activation.

Despite the significant inhibition of the increase in plasma renin activity and Ang II in MI mice, aliskiren treatment did not ameliorate LV remodeling or failure after MI, with no changes being observed in infarct size, cardiomyocyte hypertrophy, or interstitial fibrosis. In contrast, a previous study demonstrated that 50 mg/kg/day of aliskiren prevented ventricular remodeling, hypertrophy, and apoptosis after MI (Westermann et al., 2008). However, for our experiments we selected a non-depressor

concentration of aliskiren (10 mg/kg/day) in order to observe its anti-hypertensive action on insulin resistance in isolation, and thus the minimal effect of aliskiren on cardiac function might have been due to the relatively small amount used. On the other hand, the mortality rate in MI mice was significantly improved by the low-dose administration of aliskiren, suggesting that the favorable effect of aliskiren on insulin resistance may lead to an improvement of outcomes in HF after MI.

In a scientific statement from the American Heart Association, ischemic heart disease has been recommended as a model of acquired dilated cardiomyopathy and HF (Houser et al., 2012). Ischemic heart disease is the most common underlying cause of HF in humans, and the MI model exhibits the structural and mechanical alterations and shares many of the neurohormonal, cellular, and molecular features of HF in humans. The role of HF in the promotion of insulin resistance has been demonstrated by several experimental models, including a pacing-induced HF model, a model of pressure-overloaded HF by transverse aortic constriction (TAC), and a model of post-MI HF by permanent ligation of the left coronary artery (Nikolaidis et al., 2004; Shimizu et al., 2012). In the present study, a major advantage of the MI model is the capacity for studying the pathological impact of ischemic etiology on insulin resistance in HF, because it is still a matter of debate whether insulin resistance enhances the risk for development of HF exclusively in patients with ischemic heart disease (Das et al., 2004; Swan et al., 1997). The present study demonstrates that HF mice exhibit systemic insulin resistance, which is characterized by increases in the plasma insulin level, HOMA index, and percent change in blood glucose after insulin load. Moreover, impaired insulin signaling also develops in the skeletal muscle of MI mice, concomitant with a decrease in insulin-stimulated serine phosphorylation of Akt and GLUT-4

translocation to the membrane. Skeletal muscle is the major organ responsible for glucose utilization, with insulin-stimulated Akt phosphorylation and GLUT4 translocation being the rate limiting steps for these processes (Krook et al., 1997). A previous study reported that the level of GLUT4 protein was decreased in the biopsied skeletal muscle of non-diabetic HF patients, in association with decreases in insulin resistance and functional severity (Doehner et al., 2010). In support of this finding, we previously reported that reduced Akt phosphorylation and GLUT4 translocation to the membrane in the skeletal muscle resulted in systemic insulin resistance in post-infarct HF mice (Fukushima et al., 2014; Ohta et al., 2011). Thus, impairments in this signaling in the skeletal muscle are likely to contribute to the systemic metabolic derangements seen in HF patients (Kinugawa et al., 2015). Importantly, treatment with aliskiren ameliorated insulin resistance in parallel with normalization of insulin signaling and NAD(P)H oxidase-derived oxidative stress in the skeletal muscle in MI mice. Aliskiren blocks the activation of RAS at the initial step of renin inhibition, and has been shown to improve glucose transport in the skeletal muscle tissue from renin transgenic rats (Lastra et al., 2009). Since Ang II is known to directly impair insulin signaling through NAD(P)H oxidase activation in skeletal muscle cells (Wei et al., 2006), aliskiren is considered to be an attractive therapeutic approach to ameliorate insulin resistance associated with HF. On the other hand, NEFA was increased in MI mice and was normalized by aliskiren, suggesting that HF-induced lipolysis of adipose tissue is alleviated by aliskiren. Although there was no significant change in mean adipocyte area among the 4 groups, we cannot completely exclude the effect of aliskiren on other insulin-sensitive organs such as adipose tissue, because aliskiren was systemically administered by using an osmotic mini pump.

Another important finding is that local (pro)renin receptor expression rather than classical local RAS components is upregulated in the skeletal muscle in MI mice, which is normalized by aliskiren treatment. Activation of (pro)renin receptors has been shown to enhance the enzymatic activity of prorenin, in association with the pathogenesis of cardiovascular and renal injuries in hypertension, diabetes, and heart failure (Fukushima et al., 2013; Ichihara et al., 2006a; Ichihara et al., 2006b). In addition, we recently reported that upregulated (pro)renin receptor expression enhances Ang II production and oxidative stress, resulting in insulin resistance in HF mice after MI (Fukushima et al., 2014). Interestingly, the present study clearly demonstrates that administration of aliskiren to MI mice attenuates the increase in both (pro)renin receptor expression and the resulting Ang II content in the skeletal muscle. Since aliskiren can bind not only to circulating activated renin, but also to (pro)renin receptor-bound renin and prorenin (Biswas et al., 2010), the binding of aliskiren to renin and prorenin may influence both local levels of (pro)renin receptor as well as Ang II in the skeletal muscle. Indeed, a recent study has shown that aliskiren inhibits the prorenin-induced increase in intracellular Ang II of human podocytes (Sakoda et al., 2010). Therefore, these results suggest the potential impact of aliskiren on (pro)renin receptor-mediated local RAS activation and subsequent oxidative stress, rather than systemic or classical local RAS components. However, it was difficult to clarify the sites of aliskiren activity in the present study due to the dual efficacy of this agent. A major limitation in the present study was thus the lack of more definitive mechanistic experiments to delineate the causal effect of aliskiren on (pro)renin receptors, oxidative stress, and insulin resistance. Further studies on the modulation of (pro)renin receptors under aliskiren treatment are needed.

In conclusion, aliskiren ameliorated insulin resistance associated with HF by improving insulin signaling, at least in part by inhibiting systemic and (pro)renin receptor-mediated local RAS activation and subsequent NAD(P)H oxidase-induced O_2^- production in the skeletal muscle. The current study provides further support for targeting systemic RAS and (pro)renin receptor-mediated local RAS as a therapeutic intervention to improve insulin action in the skeletal muscle in the setting of HF-associated insulin resistance.

Disclosures

No conflicts of interest

References

AlZadjali, M.A., Godfrey, V., Khan, F., Choy, A., Doney, A.S., Wong, A.K., Petrie, J.R., Struthers, A.D., Lang, C.C., 2009. Insulin resistance is highly prevalent and is

associated with reduced exercise tolerance in nondiabetic patients with heart failure. J. Am. Coll. Cardiol. 53, 747-753.

Biswas, K.B., Nabi, A.H., Arai, Y., Nakagawa, T., Ebihara, A., Ichihara, A., Watanabe, T., Inagami, T., Suzuki, F., 2010. Aliskiren binds to renin and prorenin bound to (pro)renin receptor in vitro. Hypertens. Res. 33, 1053-1059.

Das, S.R., Drazner, M.H., Yancy, C.W., Stevenson, L.W., Gersh, B.J., Dries, D.L., 2004. Effects of diabetes mellitus and ischemic heart disease on the progression from asymptomatic left ventricular dysfunction to symptomatic heart failure: a retrospective analysis from the Studies of Left Ventricular Dysfunction (SOLVD) Prevention trial. Am. Heart J. 148, 883-888.

de Resende, M.M., Kauser, K., Mill, J.G., 2006. Regulation of cardiac and renal mineralocorticoid receptor expression by captopril following myocardial infarction in rats. Life Sci. 78, 3066-3073.

Doehner, W., Gathercole, D., Cicoira, M., Krack, A., Coats, A.J., Camici, P.G., Anker, S.D., 2010. Reduced glucose transporter GLUT4 in skeletal muscle predicts insulin resistance in non-diabetic chronic heart failure patients independently of body composition. Int. J. Cardiol. 138, 19-24.

Doehner, W., Rauchhaus, M., Ponikowski, P., Godsland, I.F., von Haehling, S., Okonko, D.O., Leyva, F., Proudler, A.J., Coats, A.J., Anker, S.D., 2005. Impaired insulin sensitivity as an independent risk factor for mortality in patients with stable chronic heart failure. J. Am. Coll. Cardiol. 46, 1019-1026.

Fogari, R., Zoppi, A., Mugellini, A., Lazzari, P., Derosa, G., 2010. Different effects of aliskiren and losartan on fibrinolysis and insulin sensitivity in hypertensive patients with metabolic syndrome. Horm. Metab. Res. 42, 892-896.

Fukushima, A., Kinugawa, S., Homma, T., Masaki, Y., Furihata, T., Abe, T., Suga, T., Takada, S., Kadoguchi, T., Okita, K., Matsushima, S., Tsutsui, H., 2013. Increased plasma soluble (pro)renin receptor levels are correlated with renal dysfunction in patients with heart failure. Int. J. Cardiol. 168, 4313-4314.

Fukushima, A., Kinugawa, S., Takada, S., Matsushima, S., Sobirin, M.A., Ono, T., Takahashi, M., Suga, T., Homma, T., Masaki, Y., Furihata, T., Kadoguchi, T., Yokota, T., Okita, K., Tsutsui, H., 2014. (Pro)renin receptor in skeletal muscle is involved in the development of insulin resistance associated with postinfarct heart failure in mice. Am J Physiol Endocrinol Metab 307, E503-514.

Gheorghiade, M., Bohm, M., Greene, S.J., Fonarow, G.C., Lewis, E.F., Zannad, F., Solomon, S.D., Baschiera, F., Botha, J., Hua, T.A., Gimpelewicz, C.R., Jaumont, X., Lesogor, A., Maggioni, A.P., Investigators, A., Coordinators, 2013. Effect of aliskiren on postdischarge mortality and heart failure readmissions among patients hospitalized for heart failure: the ASTRONAUT randomized trial. JAMA 309, 1125-1135.

Gradman, A.H., Traub, D., 2007. The efficacy of aliskiren, a direct renin inhibitor, in the treatment of hypertension. Reviews in cardiovascular medicine 8 Suppl 2, S22-30.

Houser, S.R., Margulies, K.B., Murphy, A.M., Spinale, F.G., Francis, G.S., Prabhu, S.D., Rockman, H.A., Kass, D.A., Molkentin, J.D., Sussman, M.A., Koch, W.J., American Heart Association Council on Basic Cardiovascular Sciences, C.o.C.C., Council on Functional, G., Translational, B., 2012. Animal models of heart failure: a scientific statement from the American Heart Association. Circ. Res. 111, 131-150.

Ichihara, A., Kaneshiro, Y., Takemitsu, T., Sakoda, M., Suzuki, F., Nakagawa, T., Nishiyama, A., Inagami, T., Hayashi, M., 2006a. Nonproteolytic activation of prorenin contributes to development of cardiac fibrosis in genetic hypertension. Hypertension 47, 894-900.

Ichihara, A., Suzuki, F., Nakagawa, T., Kaneshiro, Y., Takemitsu, T., Sakoda, M., Nabi, A.H.M.N., Nishiyama, A., Sugaya, T., Hayashi, M., Inagami, T., 2006b. Prorenin Receptor Blockade Inhibits Development of Glomerulosclerosis in Diabetic Angiotensin II Type 1a Receptor–Deficient Mice. J. Am. Soc. Nephrol. 17, 1950-1961.

Ingelsson, E., Sundstrom, J., Arnlov, J., Zethelius, B., Lind, L., 2005. Insulin resistance and risk of congestive heart failure. JAMA 294, 334-341.

Iwai, M., Kanno, H., Tomono, Y., Inaba, S., Senba, I., Furuno, M., Mogi, M., Horiuchi, M., 2010. Direct renin inhibition improved insulin resistance and adipose tissue dysfunction in type 2 diabetic KK-A(y) mice. J. Hypertens. 28, 1471-1481.

Kinugawa, S., Takada, S., Matsushima, S., Okita, K., Tsutsui, H., 2015. Skeletal Muscle Abnormalities in Heart Failure. International heart journal 56, 475-484.

Kinugawa, S., Tsutsui, H., Hayashidani, S., Ide, T., Suematsu, N., Satoh, S., Utsumi, H., Takeshita, A., 2000. Treatment with dimethylthiourea prevents left ventricular remodeling and failure after experimental myocardial infarction in mice: role of oxidative stress. Circ. Res. 87, 392-398.

Krook, A., Kawano, Y., Song, X.M., Efendic, S., Roth, R.A., Wallberg-Henriksson, H., Zierath, J.R., 1997. Improved glucose tolerance restores insulin-stimulated Akt kinase activity and glucose transport in skeletal muscle from diabetic Goto-Kakizaki rats. Diabetes 46, 2110-2114.

Lastra, G., Habibi, J., Whaley-Connell, A.T., Manrique, C., Hayden, M.R., Rehmer, J., Patel, K., Ferrario, C., Sowers, J.R., 2009. Direct renin inhibition improves systemic insulin resistance and skeletal muscle glucose transport in a transgenic rodent model of tissue renin overexpression. Endocrinology 150, 2561-2568.

Lopaschuk, G.D., Ussher, J.R., Folmes, C.D., Jaswal, J.S., Stanley, W.C., 2010. Myocardial fatty acid metabolism in health and disease. Physiol. Rev. 90, 207-258.

Marchionne, E.M., Diamond-Stanic, M.K., Prasonnarong, M., Henriksen, E.J., 2012. Chronic renin inhibition with aliskiren improves glucose tolerance, insulin sensitivity, and skeletal muscle glucose transport activity in obese Zucker rats. Am J Physiol Regul Integr Comp Physiol 302, R137-142.

Matsushima, S., Kinugawa, S., Yokota, T., Inoue, N., Ohta, Y., Hamaguchi, S., Tsutsui, H., 2009. Increased myocardial NAD(P)H oxidase-derived superoxide causes the exacerbation of postinfarct heart failure in type 2 diabetes. Am J Physiol Heart Circ Physiol 297, H409-416.

Mohammad, S., Taha, A., Bamezai, R.N., Baquer, N.Z., 2006. Modulation of glucose transporter (GLUT4) by vanadate and Trigonella in alloxan-diabetic rats. Life Sci. 78, 820-824.

Nagai, Y., Ichihara, A., Nakano, D., Kimura, S., Pelisch, N., Fujisawa, Y., Hitomi, H., Hosomi, N., Kiyomoto, H., Kohno, M., Ito, H., Nishiyama, A., 2009. Possible contribution of the non-proteolytic activation of prorenin to the development of insulin resistance in fructose-fed rats. Exp. Physiol. 94, 1016-1023.

Nikolaidis, L.A., Sturzu, A., Stolarski, C., Elahi, D., Shen, Y.T., Shannon, R.P., 2004. The development of myocardial insulin resistance in conscious dogs with advanced dilated cardiomyopathy. Cardiovasc. Res. 61, 297-306.

Officers, A., Coordinators for the, A.C.R.G.T.A., Lipid-Lowering Treatment to Prevent Heart Attack, T., 2002. Major outcomes in high-risk hypertensive patients randomized to angiotensin-converting enzyme inhibitor or calcium channel blocker vs diuretic: The Antihypertensive and Lipid-Lowering Treatment to Prevent Heart Attack Trial (ALLHAT). JAMA 288, 2981-2997.

Ohta, Y., Kinugawa, S., Matsushima, S., Ono, T., Sobirin, M.A., Inoue, N., Yokota, T., Hirabayashi, K., Tsutsui, H., 2011. Oxidative stress impairs insulin signal in skeletal muscle and causes insulin resistance in postinfarct heart failure. Am J Physiol Heart Circ Physiol 300, H1637-1644.

Okita, K., Kinugawa, S., Tsutsui, H., 2013. Exercise intolerance in chronic heart failure--skeletal muscle dysfunction and potential therapies. Circ J 77, 293-300.

Sakoda, M., Ichihara, A., Kurauchi-Mito, A., Narita, T., Kinouchi, K., Murohashi-Bokuda, K., Saleem, M.A., Nishiyama, A., Suzuki, F., Itoh, H., 2010. Aliskiren Inhibits Intracellular Angiotensin II Levels Without Affecting (Pro)renin Receptor Signals in Human Podocytes. Am. J. Hypertens. 23, 575-580.

Satofuka, S., Ichihara, A., Nagai, N., Koto, T., Shinoda, H., Noda, K., Ozawa, Y., Inoue, M., Tsubota, K., Itoh, H., Oike, Y., Ishida, S., 2007. Role of Nonproteolytically Activated Prorenin in Pathologic, but Not Physiologic, Retinal Neovascularization. Invest. Ophthalmol. Vis. Sci. 48, 422-429.

Shimizu, I., Yoshida, Y., Katsuno, T., Tateno, K., Okada, S., Moriya, J., Yokoyama, M., Nojima, A., Ito, T., Zechner, R., Komuro, I., Kobayashi, Y., Minamino, T., 2012. p53-induced adipose tissue inflammation is critically involved in the development of insulin resistance in heart failure. Cell Metab 15, 51-64.

Sobirin, M.A., Kinugawa, S., Takahashi, M., Fukushima, A., Homma, T., Ono, T., Hirabayashi, K., Suga, T., Azalia, P., Takada, S., Taniguchi, M., Nakayama, T., Ishimori, N., Iwabuchi, K., Tsutsui, H., 2012. Activation of natural killer T cells ameliorates postinfarct cardiac remodeling and failure in mice. Circ. Res. 111, 1037-1047.

Solomon, S.D., Shin, S.H., Shah, A., Skali, H., Desai, A., Kober, L., Maggioni, A.P., Rouleau, J.L., Kelly, R.Y., Hester, A., McMurray, J.J., Pfeffer, M.A., 2011. Effect of the direct renin inhibitor aliskiren on left ventricular remodelling following myocardial infarction with systolic dysfunction. Eur. Heart J. 32, 1227-1234.

Swan, J.W., Anker, S.D., Walton, C., Godsland, I.F., Clark, A.L., Leyva, F., Stevenson, J.C., Coats, A.J., 1997. Insulin resistance in chronic heart failure: relation to severity and etiology of heart failure. J. Am. Coll. Cardiol. 30, 527-532.

Takada, S., Hirabayashi, K., Kinugawa, S., Yokota, T., Matsushima, S., Suga, T., Kadoguchi, T., Fukushima, A., Homma, T., Mizushima, W., Masaki, Y., Furihata, T., Katsuyama, R., Okita, K., Tsutsui, H., 2014. Pioglitazone ameliorates the lowered exercise capacity and impaired mitochondrial function of the skeletal muscle in type 2 diabetic mice. Eur. J. Pharmacol. 740, 690-696.

Takada, S., Kinugawa, S., Hirabayashi, K., Suga, T., Yokota, T., Takahashi, M., Fukushima, A., Homma, T., Ono, T., Sobirin, M.A., Masaki, Y., Mizushima, W., Kadoguchi, T., Okita, K., Tsutsui, H., 2013. Angiotensin II receptor blocker improves the lowered exercise capacity and impaired mitochondrial function of the skeletal muscle in type 2 diabetic mice. J. Appl. Physiol. 114, 844-857.

Wei, Y., Sowers, J.R., Nistala, R., Gong, H., Uptergrove, G.M., Clark, S.E., Morris, E.M., Szary, N., Manrique, C., Stump, C.S., 2006. Angiotensin II-induced NADPH

oxidase activation impairs insulin signaling in skeletal muscle cells. J. Biol. Chem. 281, 35137-35146.

Westermann, D., Riad, A., Lettau, O., Roks, A., Savvatis, K., Becher, P.M., Escher, F., Jan Danser, A.H., Schultheiss, H.P., Tschope, C., 2008. Renin inhibition improves cardiac function and remodeling after myocardial infarction independent of blood pressure. Hypertension 52, 1068-1075.

Wilson, J.R., Mancini, D.M., Dunkman, W.B., 1993. Exertional fatigue due to skeletal muscle dysfunction in patients with heart failure. Circulation 87, 470-475.

Witteles, R.M., Tang, W.H., Jamali, A.H., Chu, J.W., Reaven, G.M., Fowler, M.B., 2004. Insulin resistance in idiopathic dilated cardiomyopathy: a possible etiologic link. J. Am. Coll. Cardiol. 44, 78-81.

Yokota, T., Kinugawa, S., Hirabayashi, K., Matsushima, S., Inoue, N., Ohta, Y., Hamaguchi, S., Sobirin, M.A., Ono, T., Suga, T., Kuroda, S., Tanaka, S., Terasaki, F., Okita, K., Tsutsui, H., 2009. Oxidative stress in skeletal muscle impairs mitochondrial respiration and limits exercise capacity in type 2 diabetic mice. Am J Physiol Heart Circ Physiol 297, H1069-1077.

Figure legends

Fig. 1. (**A**) Representative high-power photomicrographs of LV cross-sections stained with Masson's trichrome from Sham, Sham+Aliskiren, MI, and MI+Aliskiren mice, and summary data of myocyte cross-sectional area and collagen volume fraction (**B**) in the 4 groups of mice (n=5). Scale bar, 25 μm. Data are expressed as means ± S.E.M. *$P <$ 0.05 vs. Sham.

Fig. 2. (**A**) Percent changes in blood glucose during intraperitoneal glucose tolerance test in Sham (open circles, n=10), Sham+Aliskiren (open squares, n=8), MI (closed circles, n=10), and MI+Aliskiren (closed squares, n=9) mice and (**B**) area under the curve (AUC). Data are expressed as means ± S.E.M. AUC, area under the curve. *$P <$ 0.05 vs. Sham, †$P < 0.05$ vs. MI.

Fig. 3. Representative Western blot analysis (**upper panels**) and the summary data (**lower panels**) for p-Akt/Akt (**A**), and membrane fraction/cytosolic fractions of GLUT4 (**B**) in insulin-stimulated skeletal muscle from Sham, Sham+Aliskiren, MI, and MI+Aliskiren mice (n=4-6 each). Data are expressed as means ± S.E.M. p-Akt, serine-phosphorylation of Akt; GLUT4, glucose transporter 4. *$P < 0.05$ vs. Sham, †$P < 0.05$ vs. MI.

Fig. 4. Plasma renin activity (**A**) and plasma Ang II (**B**) from Sham, Sham+Aliskiren, MI, and MI+Aliskiren mice (n=5-7 each group). Data are expressed as means ± S.E.M. Ang II, angiotensin II. *$P < 0.05$ vs. Sham, †$P < 0.05$ vs. MI.

Fig. 5. Gene expression of Cathepsin D, (pro)renin receptor, angiotensinogen, angiotensin converting enzyme (ACE), and angiotensin II (Ang II) type1 receptor in the skeletal muscle obtained from Sham, Sham+Aliskiren, MI, and MI+Aliskiren mice (n=6-8, each group). Data are expressed as means ± S.E.M. ACE indicates angiotensin converting enzyme; Ang II, angiotensin II. *P < 0.05 vs. Sham, †P < 0.05 vs. MI.

Fig. 6. (**A, left**) Representative immunohistochemical staining for (pro)renin receptor in the skeletal muscle tissue from the Sham, MI, and MI+Aliskiren groups. (**A, right**) Representative Western blot analysis (**upper panel**) and the summary data (**lower panel**) for (pro)renin receptor in the skeletal muscle from the Sham, MI, and MI+Aliskiren groups (n=10 each). (**B**) Angiotensin (Ang) II content in the skeletal muscle from the Sham, MI, and MI+Aliskiren groups (n=8 each). Data are expressed as means ± S.E.M. Ang II, angiotensin II. *P < 0.05 vs. Sham, †P < 0.05 vs. MI.

Fig. 7. (**A**) O_2^- production (**left**) and NAD(P)H oxidase activity (**right**) in the skeletal muscle obtained from Sham, Sham+Aliskiren, MI, and MI+Aliskiren mice (n=5-7 for each group). (**B**) Gene expression of NAD(P)H oxidase subunits including Nox 2, p22^{phox}, and p47^{phox} in the skeletal muscle obtained from Sham, Sham+Aliskiren, MI, and MI+Aliskiren mice (n=5-7 for each group). Data are expressed as means ± S.E.M. RLU, relative light unit. *P < 0.05 vs. Sham, †P < 0.05 vs. MI.

Table 1. Animal Characteristics

	Sham	Sham + Aliskiren	MI	MI + Aliskiren
N	10	10	11	11
Body and organ weight				
BW, g	25.9±0.3	26.3±0.4	25.8±0.3	26.0±0.5
Heart weight, mg	135.7±2.3	138.9±2.4	215.2±6.2[a]	204.6±12[a]
Lung weight/BW, mg/g	5.3±0.0	5.3±0.1	8.2±0.9[a]	7.8±0.9[a]
SKM weight/BW, mg/g	15.9±0.2	15.9±0.2	16.7±0.2	15.9±0.3
Echocardiography				
Heart rate, beats/min	427±15	410±26	476±19	474±30
LV EDD, mm	3.7±0.1	3.5±0.1	5.1±0.1[a]	4.9±0.1[a]
LV ESD, mm	2.4±0.1	2.3±0.1	4.4±0.1[a]	4.2±0.1[a]
Fractional shortening, %	33.8±1.1	33.1±2.8	14.1±0.5[a]	17.2±2.6[a]
AWT, mm	0.78±0.01	0.75±0.01	0.65±0.02[a]	0.71±0.02
PWT, mm	0.83±0.02	0.78±0.03	1.08±0.03[a]	1.05±0.03[a]
Hemodynamics				
Heart rate, beats/min	448±19	465±19	448±12	460±20
Mean aortic pressure, mmHg	78±2	72±2	78±2	72±2
LV EDP, mmHg	0.7±0.1	0.9±0.1	6.4±1.1[a]	5.4±1.6[a]
LV +dP/dt, mmHg/s	10409±830	10344±956	7382±596[a]	7045±750[a]
LV -dP/dt, mmHg/s	-7222±571	-7503±439	-4560±273[a]	-4632±419[a]

Histology

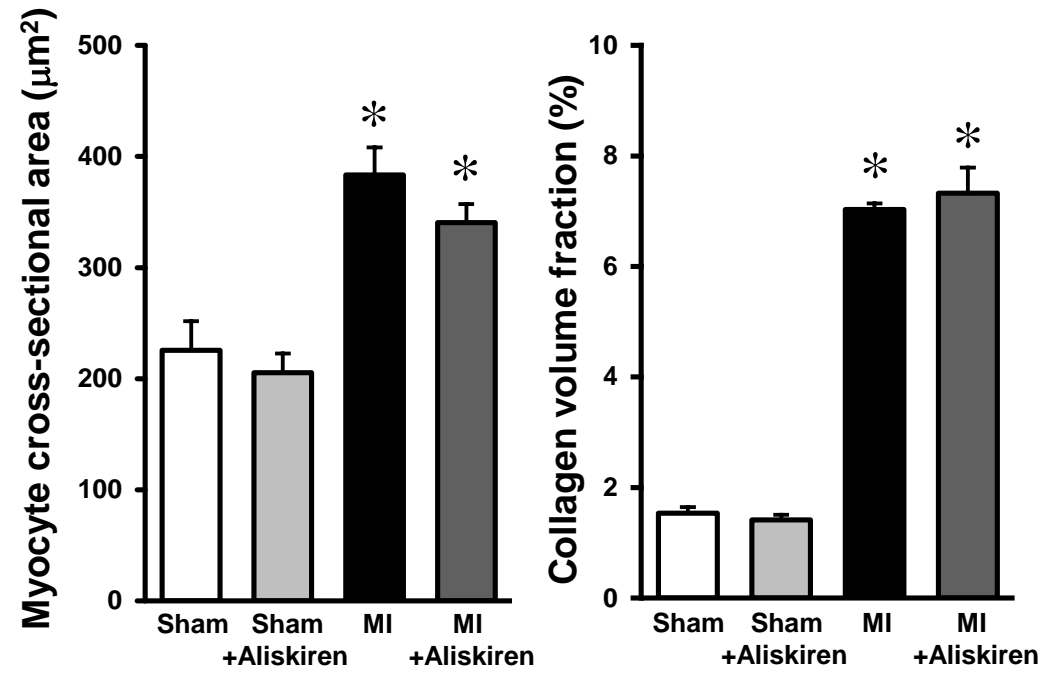|				
Infarct size, %	NA	NA	55.5 ± 2.5^{a}	52.8 ± 5.1^{a}

Values are means $\pm$ S.E.M.; *N*, number of animals. MI, myocardial infarction; LV, left ventricle; EDD, end-diastolic diameter; ESD, end-systolic diameter; AWT, anterior wall thickness; PWT, posterior wall thickness; EDP, end-diastolic pressure; +dP/d*t*, positive change in pressure over time; -dP/d*t*, negative change in pressure over time; BW, body weight; SKM, skeletal muscle. [a] P<0.05 vs. Sham.

Table 2. Biochemical data

	Sham		Sham +Aliskiren		MI		MI +Aliskiren	
N	8		8		8		8	
Blood glucose, mg/ml	90	$\pm$ 8	98	$\pm$ 8	92	$\pm$ 11	98	$\pm$ 10
Plasma insulin, ng/ml	0.43	$\pm$ 0.09	0.44	$\pm$ 0.05	0.98	$\pm$ 0.18[a]	0.52	$\pm$ 0.08[b]
HOMA index	1.5	$\pm$ 0.4	1.8	$\pm$ 0.2	3.6	$\pm$ 0.5[a]	2.0	$\pm$ 0.5[b]
Total cholesterol, mg/dl	69	$\pm$ 10	57	$\pm$ 7	57	$\pm$ 10	66	$\pm$ 11
Triglyceride, mg/dl	61	$\pm$ 18	81	$\pm$ 23	88	$\pm$ 32	88	$\pm$ 40
NEFA, meq/l	0.46	$\pm$ 0.07	0.48	$\pm$ 0.05	0.88	$\pm$ 0.15[a]	0.46	$\pm$ 0.05[b]

Values are means $\pm$ S.E.M.; *N*, number of animals; HOMA, homeostasis model of assessment; NEFA, nonesterified fatty acid. [a] $P < 0.05$ vs. Sham. [b] $P < 0.05$ vs. MI.
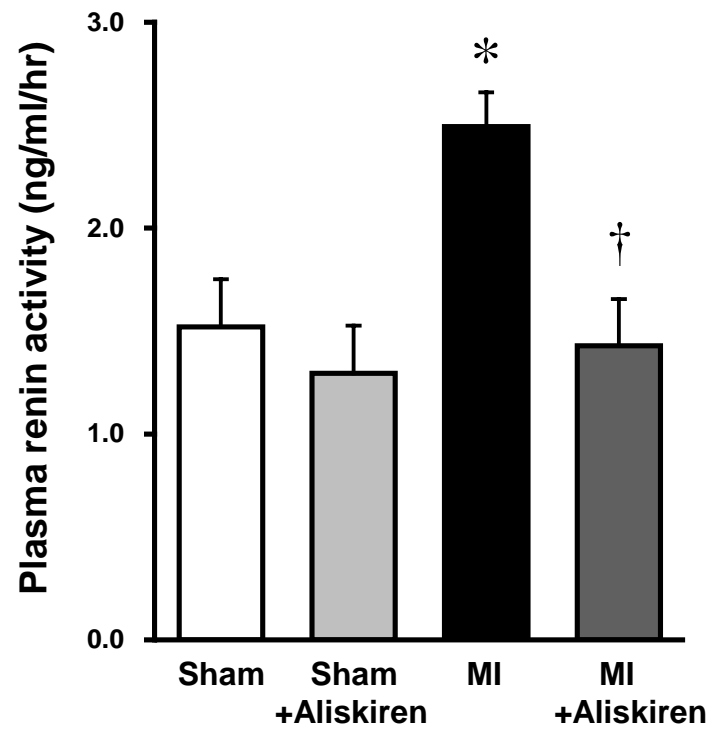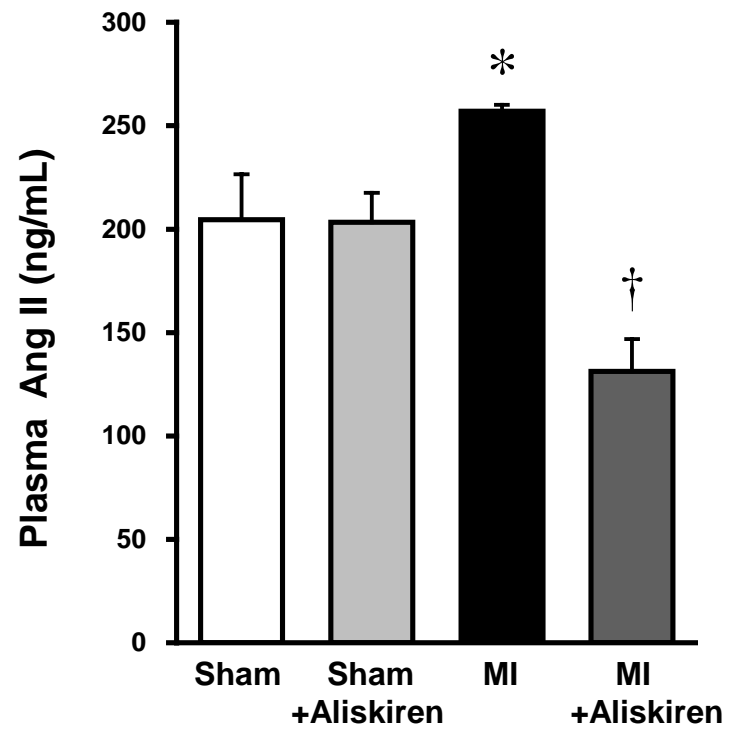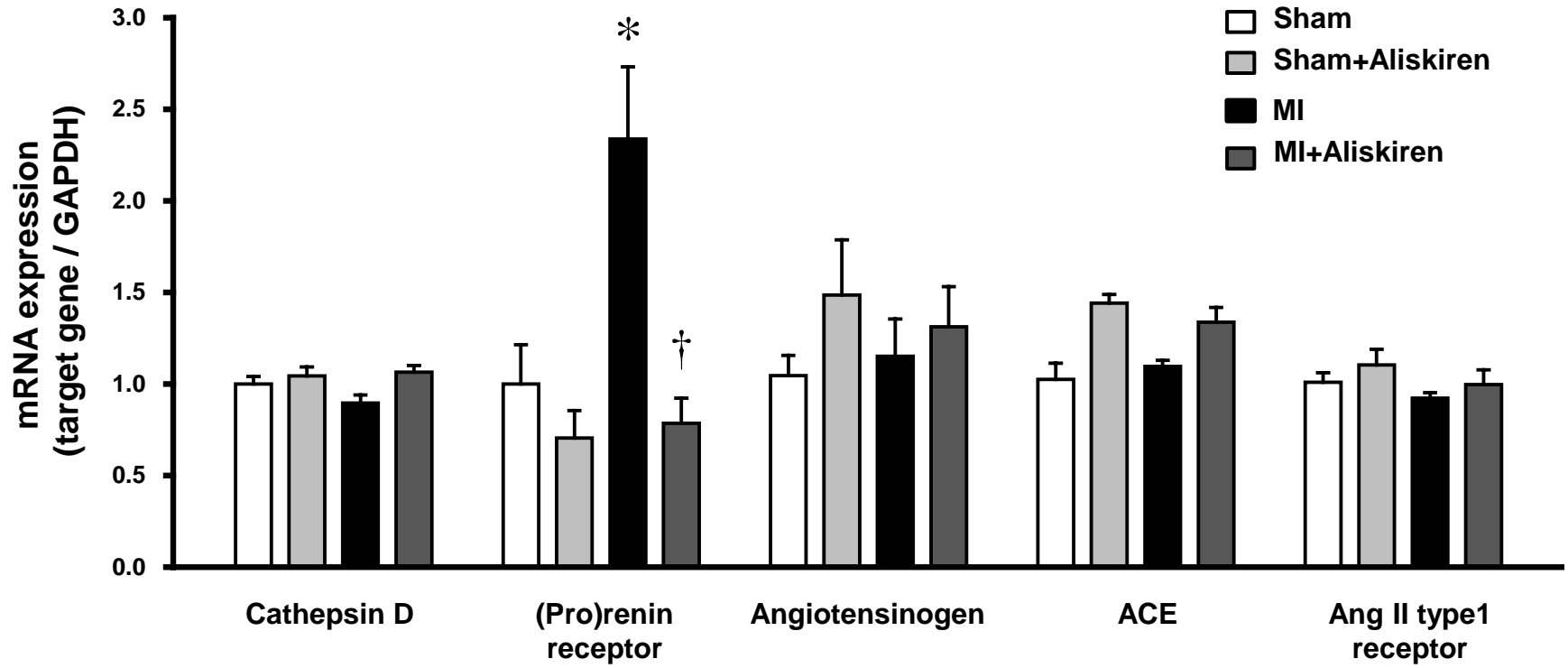
Fig. 1.

A

Sham	Sham+Aliskiren

25μm

MI	MI+Aliskiren

B

Fig. 2.

Fig. 3.

A

Sham | Sham +Aliskiren | MI | MI +Aliskiren

p-Akt

Akt

B

Sham | Sham +Aliskiren | MI | MI +Aliskiren

membrane

cytosol

Fig. 4.

A

B

Fig. 5.

Fig. 6.

A

Sham

MI

MI+Aliskiren

100μm

Sham   MI   MI +Aliskiren

(Pro)renin receptor

GAPDH

(Pro)renin receptor (ratio to GAPDH)

1.5

1.0

0.5

0.0

*

†

Sham   MI   MI +Aliskiren

B

Ang II content (pg/mg protein)

2,500

2,000

1,500

1,000

500

0

*

†

Sham   MI   MI +Aliskiren

Fig. 7.